Available online at www.sciencedirect.com

jmr&t
Journal of Materials Research and Technology
www.jmrt.com.br

Original Article

Novel application of a thermoplastic composite with improved matrix-fiber interface

S. Lopez de Armentia*, B. Enciso, G. Mokry, J. Abenojar, M.A. Martinez

Dept. of Material Science and Engineering, Univ. Carlos III de Madrid, IAAB Av. Universidad, 30, 28911 Leganes, Spain

ARTICLE INFO

Article history:
Received 20 May 2019
Accepted 7 September 2019
Available online 27 September 2019

Keywords:
Glass fiber reinforced thermoplastic
Atmospheric plasma treatment
Fiber/matrix adhesion
Impact behavior
Externally bonded reinforcement

ABSTRACT

Ornamental materials are widely used in many fields such as construction. However, they have a main issue: up to 60% of processed marble pieces break due to their low toughness. In this work, an externally bonded reinforcement which can cope with this problem is presented. It must absorb the shock energy when marble is subjected to an impact without increasing severely the production cost. A thermoplastic polymer matrix composite is proposed due to its high toughness compared with conventional thermoset polymer matrix composites. However, thermoplastics present an issue related to the adhesion with the reinforcement, therefore fibers must be treated to solve this matter. Atmospheric pressure plasma torch offers a time saving and environmental friendly solution for improving adhesion between the fibers and the matrix. Finally, when marble is reinforced with the composite an important increase in absorbed energy is found in both, Charpy and drop tower test.

1. Introduction

In the last years, the use of thermoplastics as matrix in composite materials has been growing steadily due to their recyclability and ability to be processed rapidly. They also offer improved fracture toughness and they can be joined using welding techniques. Besides, they can be easily stored for long periods of time without loss of performance or ability to be processed and it is easy to repair or remold them [1–3]. These thermoplastic composites can be used in many different industries, such as automotive, aerospace or sports [4]. In this work, they are proposed to be used as reinforcement of some brittle materials in the construction field, such as natural stone, where brittleness is one of the most important issues.

When studying composite materials, it is known that their final properties do not depend only on the properties of the separate constituents (matrix and reinforcement), but in how they interact with each other. Interaction between them occurs on the interface and can be studied from the adhesion between matrix and reinforcement. Adhesion plays an important role to transfer the stress from the matrix to the fibers, and hence it changes the final properties [5].

In order to increase the adhesion, surface properties of fibers can be modified by physical or chemical treatments. Chemical modification methods include the use of surface modifiers on fibers, as silane coupling agents or graphene oxide [6,7], compatibilizers [8], electrochemical treatment [9] or oxidation [10].

* *Corresponding author.*
E-mail: slopezar@pa.uc3m.es (S. Lopez de Armentia).
https://doi.org/10.1016/j.jmrt.2019.09.022

Physical modification methods change structural and surface properties of fibers and thereby influence the mechanical bonding with the matrix. It can be divided into macroscopic modification, such as fiber fibrillation [11] and polymer rivet [12], and microscopic methods: etching [13], plasma treatment [14] or grit blasting with micro particles [15].

Plasma treatment has been widely used to improve the adhesion of coatings and paintings on polymer surfaces [16]. It increases surface energy, wettability and adhesion capability by three different mechanisms, without affecting bulk properties. Ablation consists on the removal of organic residues as well as surface layers at a molecular level; cross-linking, meaning the formation of covalent links by the interaction between two or more radicals and surface activation due to the generation of polar groups (−COOH, −OH), which increases surface energy [17]. Besides, previous works have proved the effectiveness of this treatment on glass surfaces [18]. For this reason, atmospheric pressure plasma torch (APPT from now on) was used to treat glass fibers and improve adhesion between them and polyethylene.

One of the most important novelties of this work is the application of the composite with improved adhesion between fibers and matrix. It is related to natural stone, which has been the most commonly used material in construction, ornamentation, funerary art and a variety of artistic objects through the ages. The natural brittleness of stone results on a need to reinforce it. Specifically, consolidants are commonly used with this aim [19,20]. Glass fiber with epoxy resin is also employed in order to strengthen the marble before sawing the blocks to get slabs [21]. Thermoset composite materials are now being used worldwide for building new structures as well as for in-service structures rehabilitation. They are used as load-bearing structural components for infrastructure applications, as a corrosion-resistant alternative to external steel reinforcements [22]. However, an important drawback is found with this type of composite materials. They cannot be reused or recycled due to its irreversible cure. The thermoplastic composite developed in this work, acting as reinforcement of marble in order to reduce its fragility can cope with this issue. On polymers, brittleness depends, among others, on their crystallinity: the higher the level of crystallinity, the lower the toughness of the polymer. It is known that fibers added to a thermoplastic polymer can play a dual role: on one hand, they can act as nucleating agent, promoting higher crystallinity and on the other hand, they can restrict mobility of chains, promoting lower crystallinity [23]. When the fibers are treated, the high density of nuclei could lead to a transcrystallization process, resulting on high or low crystallinity depending on the amount and the nature of the fibers [24,25].

In this work, the effect of plasma treatment on glass fiber is studied; on one hand, from the point of view of the adhesion with the matrix and, on the other hand, the effect of this change in adhesion on the properties of the polymer.

As previously said, marble is naturally brittle. This brittleness is determined by the energy that is capable to absorb during an impact. With the externally bonded reinforcement this energy could be increased, making the toughness of the marble higher with the consequent reduction of broken pieces. In consequence this study is focused on the improvement of the adhesion between glass fiber and LDPE by plasma treatment in order to use this composite material as externally bonded reinforcement of marble pieces. Adhesion is a key factor, due to the necessity of having a good transmission of the energy through the composite.

2. Experimental part

2.1. Materials

The reinforcement was a glass fiber type E in form of bidirectional woven tape with 5 cm width supplied by Vetrotex (Alcalá de Henares, Spain). Its main components are SiO_2 (53–57 %wt.) and Al_2O_3 (12–15 %wt.). Usually, commercial glass fiber is presented with a sizing. To remove it, they were subjected to a desizing calcination at 500 °C for 1 h [26]. Calcinated fibers are used just to compare, since it is not recommended to use unsized fibers.

As matrix, a low density polyethylene (LDPE) DOW 780 E in pellets, supply by Dow Chemical (Madrid, Spain) was used.

Marble was supplied by Asociación Española del Mármol de Andalucía (AEMA). Its composition was obtained by X-Ray Fluorescence (Table 1).

2.2. Glass fiber reinforced polyethylene

2.2.1. Plasma treatment

An APPT device from Plasma Treat GmbH (Steinhagen, Germany) was utilized to treat the as-received glass fibers. It presented a torch ending nozzle that rotated at 1900 rpm, through which plasma was expelled through a circular hole onto the samples. The setup operated at a frequency of 17 kHz and a high tension discharge of 20 kV. The air plasma was generated at a working pressure of 2 bar.

In order to determine the optimum parameters of APPT (speed and nozzle-sample distance), glycerol contact angle was measured for different combinations of these parameters. Plasma treatment changes the surface energy and, consequently, wettability of surface. At least 5 drops of 4 μL of glycerol were measured for each sample.

2.2.2. Surface characterization

Dataphysics OCA15 plus goniometer and SCA20 software (DataPhysics Instruments GmbH, Filderstandt, Germany) were used in order to determine the surface energy. Deionized water, glycerol and diiodomethane contact angle measurements were used.

Owens–Wendt–Rable–Kaelble method [27] enables the determination of both dispersive and polar components of surface energy.

Van Oss, Chaudhury, Good (vOCG) [28] method is also used to determine Lifshiftz-van der Waals (LW) and acid-base (AB) contributions of surface energy. For its part, acid–base comprises two components: electron donor or basic component (γ^-) and electron acceptor (γ^+).

To study the topography Atomic Force Microscope and Scanning Electron Microscope were used. Nanoscope IV AFM (Digital Instruments, Santa Barbara, CA) with tapping mode in air at room temperature was used to take images. The probe used was NSG30 supplied by NT-MDT. With NanoScope

Table 1 – Marble composition (%wt.).

CaO	MgO	SiO_2	Al_2O_3	$BaSO_4$	P_2O_5	SO_3
60.79 ± 0.26	0.75 ± 0.17	0.37 ± 0.16	0.07 ± 0.04	0.08 ± 0.01	0.12 ± 0.01	0.04 ± 0.01

Analysis Software, roughness of the surfaces were compared. Images of scanning electron microscopy were taken by TENEO-LoVac (Eindhoven, Nederlands).

2.2.3. *Chemical characterization*

APPT and calcination effect on the chemical bonds were studied by means of attenuated total reflectance spectroscopy (ATR). The spectra were obtained using Tensor 27 Fourier Transform Infrared (FTIR) spectrometer from Bruker (BrukerOptikGmbH, Madrid, Spain), equipped with a DuraSample Diamond accessory formed by a 0.5 mm diameter diamond embedded in a ZnSe crystal. The ratio signal-to-noise is better than 8000:1 (5.4×10^{-5} noise absorbance). Spectra were recorded with a resolution of 4 cm^{-1} from 4000 to 400 cm^{-1} by taking 32 scans.

2.2.4. *Adhesion tests*

Peel tests were carried out following the ASTM D1876 – 08(2015)e1 Standard. It was modified, having the thickness (0.5 mm) and width (50 mm) of glass fiber fabric. Peel test samples were prepared by using hot plates press Fontijne Presses TPB 374 (Barendrecht, Netherland) with 140 °C, 0.5 MPa and 10 min.

T-peel test was carried out with the universal testing machine Microtest DT005 FR (Madrid, Spain) with a load cell of 1 kN. Samples consisted on two glass fiber fabrics with polyethylene between them (Fig. 1a).

For pull-off tests, aluminum dolls with a diameter of 20 mm were used. This test provides the traction resistance of the joint. They were adhered to the glass fiber by melting polyethylene between them as is shown in Fig. 1b. Then, samples were tested with the universal testing machine, according to ASTM D4541 - 17 Standard. Resistance (σ) is calculated with Eq. (1):

$$\sigma = \frac{F}{A} = \frac{F}{\pi \cdot R_{doll}{}^2} \tag{1}$$

where F is the force, A is the area and R_{doll} is the doll radius.

Finally, pull-out tests (ASTM D7913 Standard) were carried out by embedding a glass fiber roving in a LDPE pellet (Fig. 1c). It was melting in the oven at 140 °C and then it was tested to obtain the shear resistance of the fiber-matrix joint. The universal testing machine with a load cell of 50 N is used.

At least 15 specimens were prepared. With the embedded fiber length (l_{ef}), the diameter of the fiber (d_f) and the maximum force (F_{max}), interfacial shear strength (*IFSS*) τ can be calculated from Eq. (2) [29]:

$$\tau = \frac{F_{max}}{d_f \cdot \pi \cdot l_{ef}} \tag{2}$$

2.2.5. *Composite manufacturing*

Monolayer composite is manufactured by using hot plates press. Firstly, two layers of polyethylene were processed from melted pellets at 130 °C, 0.22 MPa and 10 min. Glass fiber fabric was positioned between them and the composite was manufactured at 140 °C, 0.22 MPa and 10 min. Surface energy of composite with untreated and treated fibers was calculated.

In order to study the influence of fibers and their treatment, melting point and crystallinity of LDPE in different conditions (without fibers, with untreated and with plasma treated fibers) were obtained by Differential Scanning Calorimetry. DSC 883 Mettler Toledo (Grafensee, Switzerland) equipment was used. Aluminum crucible with sample of 5–10 mg were firstly heat from −40 °C to 200 °C at 10 °C/min to remove the thermal history. Then it was cooled down to −40 °C at 20 °C/min and heated again in the same conditions. Results are analyzed in the second scan. Crystallinity (χ_c) is determined from Eq. (3):

$$\chi_c = \frac{\Delta H_c}{\Delta H_m{}^0 \cdot (1 - w_f)} \cdot 100 \tag{3}$$

where ΔH_c is the enthalpy obtained by the melting peak area, $\Delta H_m{}^o$ the melting enthalpy of LDPE 100% crystalline (288 J/g) and w_f the weight fraction of fibers [30].

2.2.6. *Mechanical tests*

Three points bending tests (ASTM D790 – 17 Standard) were carried out with the universal testing facility, with a load cell of 150 N. The three points bending device was composed of a punch and two support steel rods. The distance between supports was 25 mm. Flexural strength (σ_f) and deformation (ε_f) were determined from Eqs. (4) and (5).

$$\sigma_f = \frac{3 \cdot F \cdot L}{2 \cdot b \cdot h^2} \tag{4}$$

$$\varepsilon_f = \frac{6 \cdot s \cdot h}{L^2} \cdot 100 \tag{5}$$

F represents the applied force, L the distance between supports, b and h width and thickness of the sample, respectively and s the deflection produced.

LDPE samples and monolayer samples of untreated and treated glass fiber embedded on polyethylene matrix were tested. The flexural modulus was calculated from the slope of the elastic zone on the strain–stress curve. Besides, the stress needed to produce a 3.5% deformation on the sample was calculated. Displacement rate of the punch was set on 2 mm/min.

2.3. *Thermoplastic composite reinforced marble*

2.3.1. *Adhesion test*

Adhesion between reinforcement and marble has an important role to play in transmitting the waves formed during the impact.

In order to study adhesion between the composite and the marble, peel tests were carried out. Samples were prepared with the hot plates press (130 °C, 0.2 MPa, 10 min), after the marble surface was cleaned with acetone. Universal testing

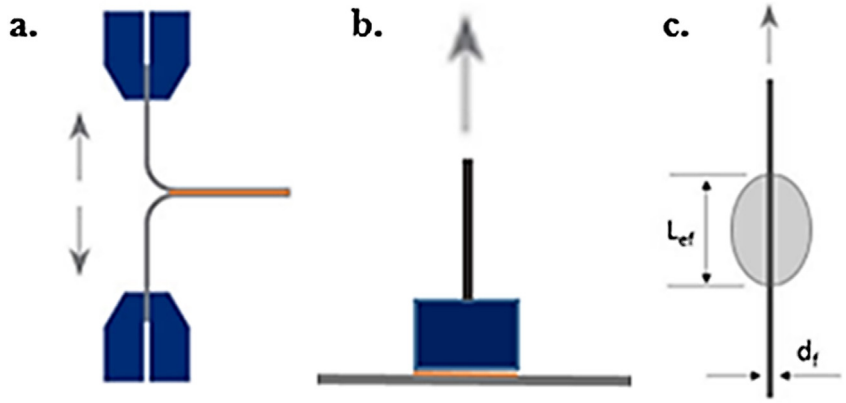

Fig. 1 – Scheme of (a) T-peel, (b) Pull-off and (c) Pull-out tests.

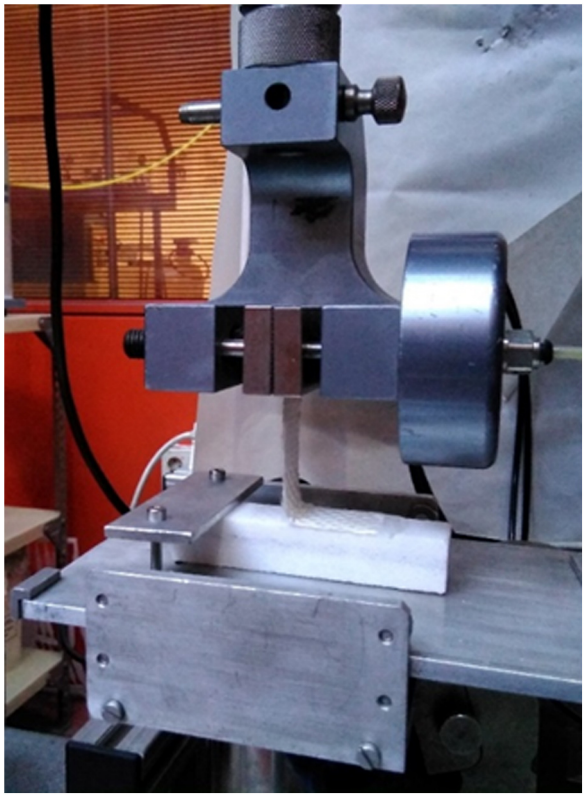

Fig. 2 – Adhesion test.

machine with 1 kN load cell equipped with a rail was used in order to have a perpendicular load throughout the test (Fig. 2).

2.3.2. *Impact tests*

When a sample is subjected to an impact, compressive waves pass through the material. They are reflected in the opposite surface as tensile waves, which are the main cause of failure in ceramic materials, such as marble. The function of the reinforcement is to absorb this energy in order to reduce the intensity of the tensile reflection, leading to a less brittle material.

In order to determine absorbed energy of the reinforced and non-reinforced marble, two different tests were done.

Table 2 – Glycerol contact angle (°) on fibers with APPT.

		Speed (m/min)		
		1	5	10
Nozzle-sample distance (mm)	4	53.8	58.4	68.7
	8	91.0	51.7	69.7

Drop tower Neurtek (Éibar, Spain) was used to determine the maximum falling height of a body of 1 kg on the material without breaking it. From this height, absorbed energy and fall speed were calculated.

On the other hand, Charpy pendulum test was carried out. Absorbed energy needed to break marble, with and without reinforcement, was measured with this test. Initial energy was fixed in 295 J. Nestor pendulum for Charpy–Izod tests was used in this work.

3. Results

3.1. *Glass fiber reinforced polyethylene*

3.1.1. *Plasma treatment optimization*

First, the parameters of the plasma are optimized: nozzle-sample distance and speed. Plasma treatments improves the wettability of a surface, hence it is possible to optimize the parameters by measuring the contact angle. In this case, it is done with glycerol. Nozzle-sample distance of 8 mm and 5 m/min gives the maximum wettability, as can be seen in Table 2.

Fibers without treatment show a contact angle of 104°. The improvement of wettability with plasma treatment is observed in Fig. 3. It is clearly observed a lower contact angle when the fiber is treated with APPT. The best condition combination is a nozzle-sample distance of 8 mm and speed of 5 m/min. With these parameters the lowest angle is obtained.

3.1.2. *Fiber surface*

3.1.2.1. Scanning electron microscopy. In order to study the plasma and the calcination effect on fiber surfaces, micrographs with SEM were taken. In these images, cleaning effect of plasma (Fig. 4b) is observed. Furthermore, when fibers are

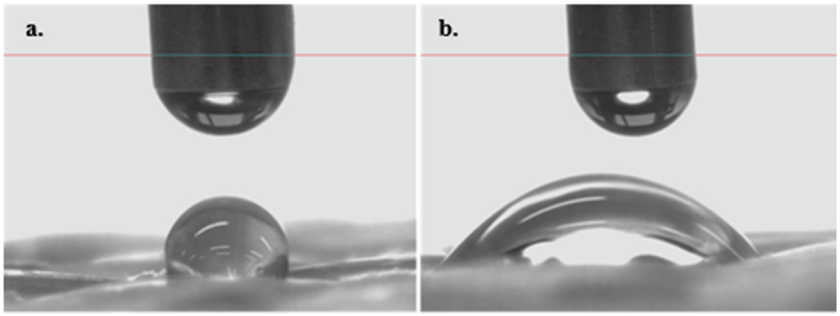

Fig. 3 – Glycerol drop on (a) untreated and (b) plasma treated fibers.

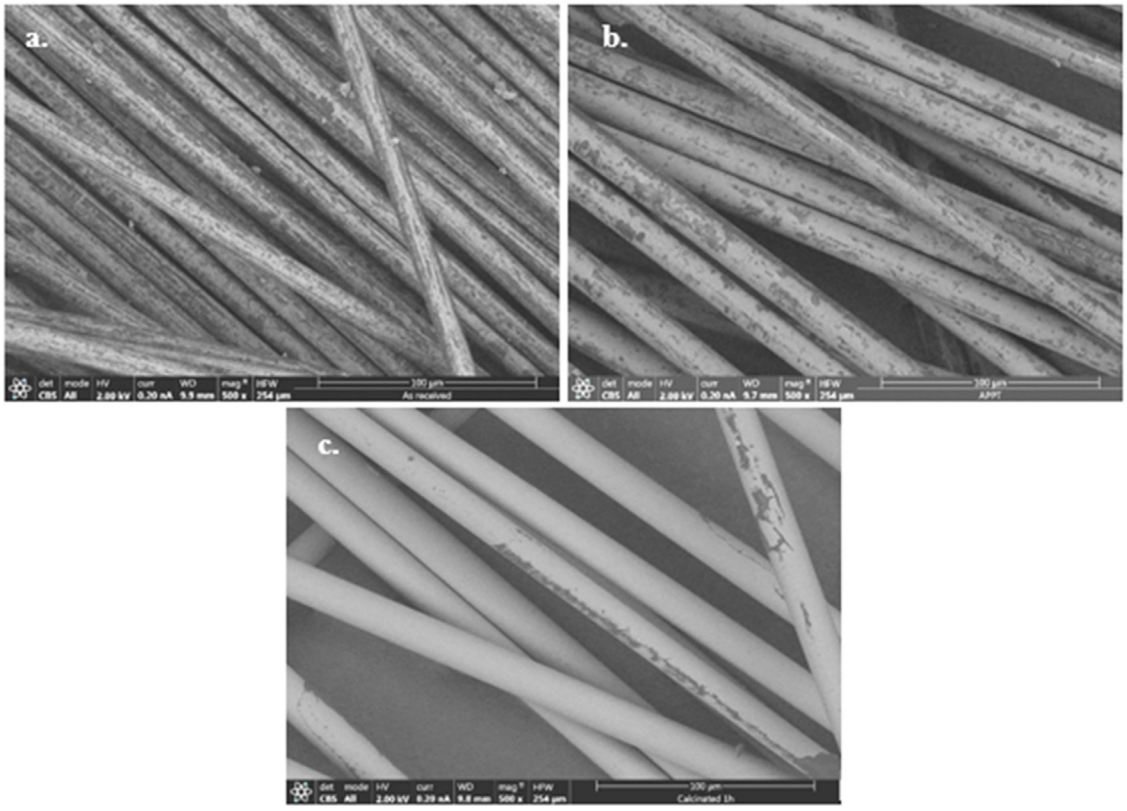

Fig. 4 – SEM images of (a) as-received, (b) treated by APPT and (c) calcinated glass fiber.

calcinated (Fig. 4c), their surface becomes cleaner and softer due to the elimination of the organic sizing, which is irregular and inhomogeneous (Fig. 4a). However, there are some parts of sizing that remains after 1 h of calcination.

It seems that plasma treatment does not remove sizing from the surface, but a more exhaustive analysis (by FTIR-ATR, for instance) is required in order to prove this.

3.1.2.2. *Atomic force microscopy.* By atomic force microscopy (AFM), fiber surfaces can be studied in nanometric scale, in this way, it is possible to verify what has been appreciated by SEM. Height images taken with AFM are shown in Fig. 5. Second order "planefit" was done in order to remove the effect of the fiber curvature. At least six profiles, with a length of 3 μm, were chosen on each sample in order to determine its roughness.

It is proved that the roughness of the surface changes when plasma treatment is applied. Surface becomes more homogeneous and the roughness decreases (Fig. 5a and b). This nanoroughness can lead to an improvement of adhesion when fibers are treated. It can be seen how the desizing process softens the surface, although remains of the sizing can still be observed (Fig. 5c).

When roughness values are compared, it can be concluded that plasma treatment, as well as the removal of the sizing, produces in both cases very flat surfaces. However, the calcinated surfaces have lower roughness than the one observed for the plasma treated fiber.

This was previously observed by other authors [27]. APPT produced etching on the sizing due to the flow of plasma. Reduction of roughness and smoothing effect of this treat-

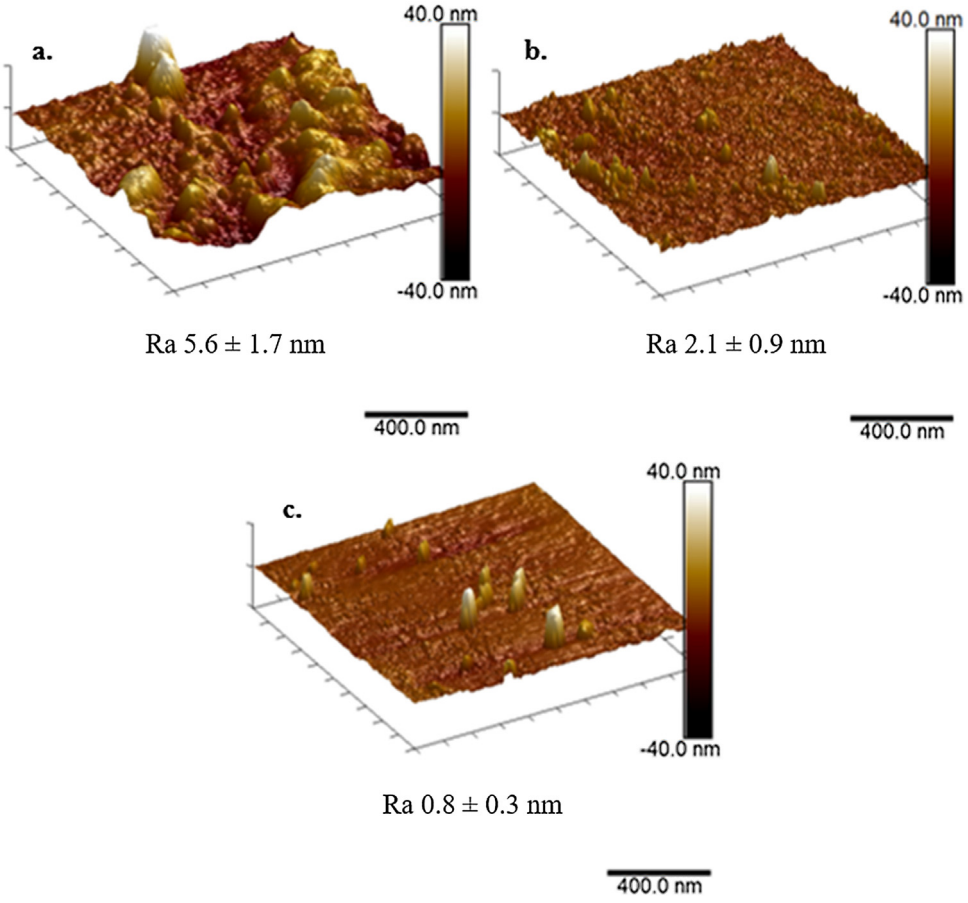

Fig. 5 – AFM micrographs of (a) as-received, (b) plasma treated and (c) calcinated glass fiber.

Table 3 – Contact angle (°) on as-received, treated and calcinated fibers.

	As-received	APPT	Calcinated
Water	112.4 ± 1.2	42.9 ± 7.2	0
Glycerol	104.5 ± 2.1	51.7 ± 4.2	32.9 ± 1.8
Diiodomethane	28.1 ± 3.5	52.2 ± 11	90.3 ± 5.8

Table 4 – Surface energy and its components of glass fiber as-received.

	As-received	APPT	Calcinated
$\gamma_{Total,\ OWRK}$	54.1 ± 1.4	53.4 ± 7.0	73.3 ± 5.1
$\gamma_{Polar,\ OWRK}$	5.4 ± 0.4	27.9 ± 5.0	62.1 ± 4.8
$\gamma_{Base,\ vOCG}$	0.1 ± 0.2	41.5 ± 11.6	68.1 ± 2.1

ment were observed on epoxy and polyester composites surfaces [31].

3.1.2.3. *Surface energy.* Wettability is a key factor on adhesion between two elements. It can be studied by contact angle measurements and surface energy calculation. These contact angle values are presented in Table 3.

An increase in wettability is produced when the treatment is applied, except for diiodomethane. This is due to the dispersive character of this liquid, while plasma affects the polar component of surface energy.

When sizing is removed and the glass surface is exposed, contact angles change completely. The wettability values observed on the sizing polymer as compared to the bare glass surface are very different, due to low surface energy of polymers, in contrast with high energy of ceramic and glass.

From these data, surface energy is calculated. OWRK and acid-base methods are used to calculate the most significant components. These components can be seen in Table 4.

It is observed how plasma treatment increases the polar component of glass fiber due to the incorporation of polar groups (C=O, C–O, etc.) on the surface, which presents dispersive nature when untreated. This increase in polarity was reported previously [31]. Furthermore, basic component rises with APPT, which leads to think that the introduced groups are those that present electron-donor character: amine, imine, ketone, ester, ether or alcohol functionalities [32].

On the other hand when the sizing is removed from the glass surface, the polar and basic character corresponds with glass [18]. This polar and electron donor character is related to the chemical structure of glass (SiO^-).

3.1.2.4. *Infrared spectroscopy.* Spectra and the identification of the peaks are presented in Fig. 6 and Table 5, respectively. Peaks corresponding to the sizing (light rectangles in Fig. 6) appear around 2800–2900 cm^{-1} ($-CH_2$ and $-CH_3$ bonds) [33] and at 1730 cm^{-1} (carbonyl groups). This peak at 1730 cm^{-1}

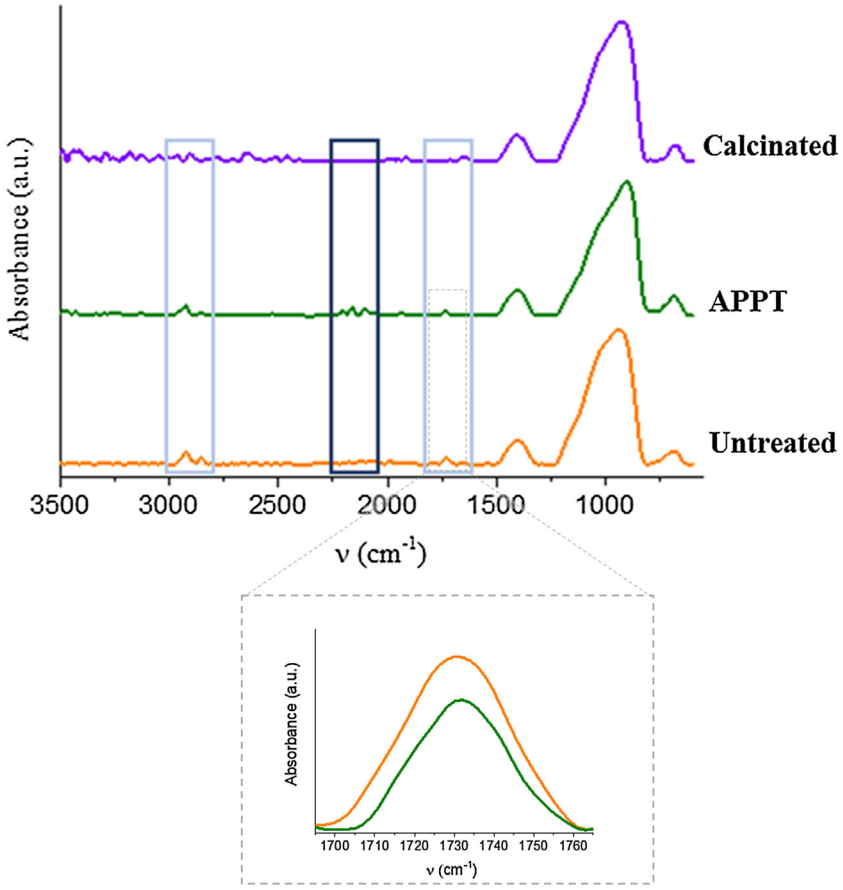

Fig. 6 – FTIR-ATR spectra of as-received, treated and calcinated fiber.

Table 5 – Asignation of peaks of untreated, APPT treated and calcinated fibers spectra.

ν (cm^{-1}) UT	ν (cm^{-1}) APPT	ν (cm^{-1}) calcinated	Asignation
700	700	700	Si–O [6]
800–1200	800–1200	800–1200	$SiOCH_3$, SiOC, SiOSi [30,34]
1730	1730	–	C═O [31]
–	2100–2160	–	$CO–CHN_2$ [35]
2850	2850	–	$–CH_2$ [30]
2920	2920	–	$–CH_3$ [30]

corresponds to the polar component of the wax present in the sizing [36].

Untreated and treated fibers spectra show these peaks, which disappear when fibers are calcinated due to the removal of the sizing. It has been observed previously by other authors when fibers were heat-cleaned [37]. With these results, and together with SEM and AFM characterization, it can be concluded that sizing is almost completely removed from the surface.

When fibers are treated with APPT bands at 2800–2900 cm^{-1} do not disappear, allowing to conclude that sizing is not removed with this treatment. Effect of plasma appears at 2100–2160 cm^{-1} (dark rectangle in Fig. 6). These bands are due to diazoketone ($–CO–CHN_2$) formed when introducing polar groups (nitrogen and oxygen) with atmospheric plasma. The introduction of these elements with the treatment was previously observed by X-ray photoelectron spectroscopy (XPS) [32,37]. Ketone groups explain the basic character of the surface energy when fibers are treated with atmospheric plasma. Plasma effect is also observed in the band at 1730 cm^{-1}, but this peak appears overlapped with the wax of the sizing. In spite of the double contribution in this peak (wax and plasma), the area of this peak is reduced when plasma is applied, so it seems that the treatment reduces the amount of wax present on the fiber surface.

Finally, groups due to fibers (Si—O—Si, Si—O) appear between 800 and 1200 cm^{-1} and 700 cm^{-1}, respectively. Overlapped with them, between 800 and 1200 cm^{-1}, the fiber-sizing bonds, and peaks of coupling agent silane, appear.

3.1.3. *Adhesion tests*

Peel tests offer an advantage compared with other tests. They allow to evaluate quantitative and qualitatively the joint, as these results show the peel resistance and the type of failure.

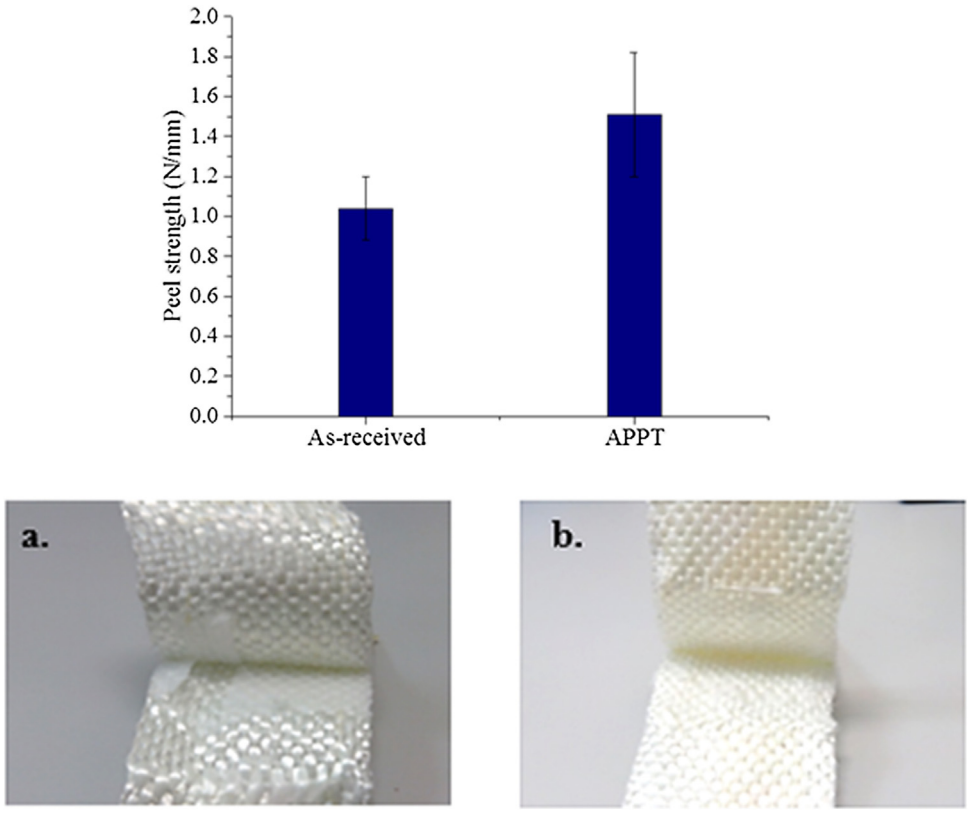

Fig. 7 – (up) Peel strength and (down) failure of polyethylene with (a) as-received and (b) APPT treated fibers.

Fig. 7 shows peel resistance when the fiber is both treated and untreated. An increase of more than 45% is produced when the joint with treated fiber is subjected to peel stress. This is due to the cleaning and elimination of low cohesion superficial layers when plasma is applied. By AFM it has also been observed a more homogeneous surface, which promotes adhesion (Fig. 5b).

In Fig. 7 down it is shown the type of failure produced when fibers are untreated (Fig. 7a) and treated with APPT (Fig. 7b). Failure mode is cohesive with plasma treatment, being adhesive without treatment. It indicates the good adhesion between matrix and reinforcement when fibers are treated.

Pull-off tests were carried out by using an aluminum doll. With doll radius, pull-off resistance was calculated, as can be seen in Fig. 8a. Pull-off adhesion improves significantly, increasing the resistance eight times when fibers are treated. However, in all cases, failure is produced in the interface between the aluminum doll and the polyethylene, therefore suggesting that adhesion between polyethylene and fiber would present higher values.

Finally, pull-out tests reveal an increase in adhesion of 35% when treatment is applied. Deviations of these results are very important, but using t student it can be concluded that, with 90% confidence, adhesion with the treatment is higher than without it. Results are shown in Fig. 8b. With these tests, it is shown how plasma treatment affects the interface by improving the adhesion from chemical and mechanical anchoring.

3.1.4. *Composite manufacturing*

Monolayer composite (GF-LDPE) is manufactured by using hot plates press. When surface energy of composite is calculated, it is observed that adding fibers, as well as treated fibers, results in drastic changes (Table 6).

LDPE shows dispersive character, which corresponds to the non-polar molecules of the polymer attracted by London forces. These forces appear in non-polar polymers, such as elastomers and soft thermoplastic polymers [38].

When the fibers are added without treatment, the surface energy of the composite increases due to an increment in the polar component; base component also increases. However if the fibers are treated, polar component of the composite presents the same value that LDPE, besides they do not present any base component. However, total surface energy increases.

In the case of untreated fiber, with the application of heat, wax of the sizing migrates to the surface, being the responsible of the high polar component. When fibers are treated, the wax is removed from their surface and the polar component of the final composite is reduced.

Other changes on the polyethylene when fibers are untreated or treated can be seen by DSC analysis. Table 7 shows crystallinity of polyethylene and melting temperature for LDPE and composites. Untreated glass fibers act as nucleating agent whilst long fibers present a preferential direction, which facilitates crystals growth. APPT fibers reinforced polyethylene shows the lowest value of crystallinity, which is due to the transcrystallization process [24,25]. Treated fibers have an activated surface providing a large number of

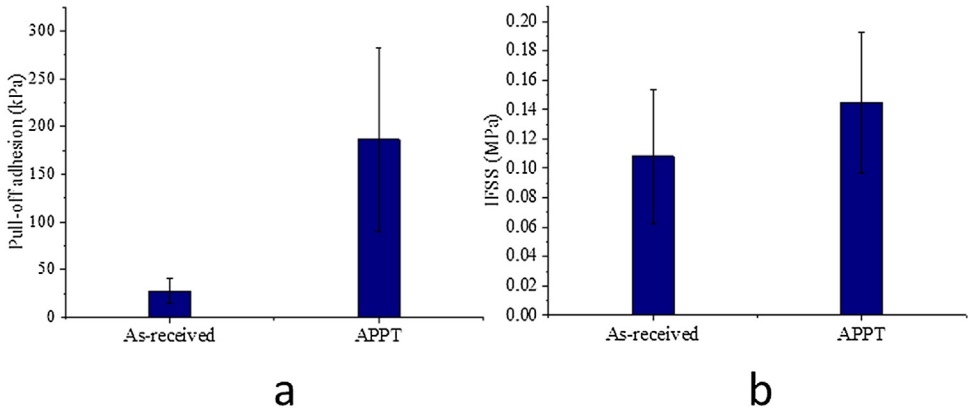

Fig. 8 – (a) Pull-off and (b) pull-out adhesion.

Table 6 – Surface energy and its components.

	LDPE	LDPE + untreated GF	LDPE + APPT GF
$\gamma_{Total, OWRK}$	28.3 ± 0.8	36.1 ± 2.9	44.9 ± 3.6
$\gamma_{Polar, OWRK}$	3.8 ± 0.4	23.5 ± 1.6	3.1 ± 3.2
$\gamma_{Base, vOCG}$	5.6 ± 1.7	42.4 ± 11.7	0.0 ± 0.0

Table 7 – Crystallinity and melting temperature for LDPE and composites.

	χ_c (%) ± 2	T_m (°C) ± 2
LDPE	15	113
LDPE + untreated GF	27	114
LDPE + APPT GF	14	112

nucleation points. They block spherulites growth except in perpendicular direction where other fibers and spherulites are found, which blocks perpendicular growth [23].

3.1.5. *Flexural tests*

Results of three points bending tests on GF-LDPE were presented in Fig. 9. All samples subjected to the bending test are more flexible than the total travel of the machine therefore exceeding its measuring limits.

It can be seen how the presence of untreated fibers in the matrix does not present an impact in the flexural modulus (Fig. 9a), but the stress at 3.5% strain is higher (Fig. 9b). This can be explained because the interface is weak but it needs a certain force to be broken. Once broken, forces are supported only by the matrix and the modulus is given by polyethylene. Furthermore, when fibers are treated and the interface is improved, an increase is observed in both, modulus and stress. It can be seen that an interphase with good properties is crucial for improving the mechanical properties of the composite.

Previous studies with basalt fibers and PBT did not find any differences in flexural modulus, between untreated fibers and the ones that were treated with silane coupling agent [39]. However, in this work, a significant improvement on flexural modulus when fibers are treated is observed.

3.2. *Marble reinforced with thermoplastic composite*

3.2.1. *Marble-composite adhesion*

Peel test allows to determine adhesion qualitatively, studying the kind of failure, and quantitatively. When the composite with untreated fibers is adhered to the marble, it is found that the joint does not present any resistance due to the presence of the wax on the composite surface. However, with treated

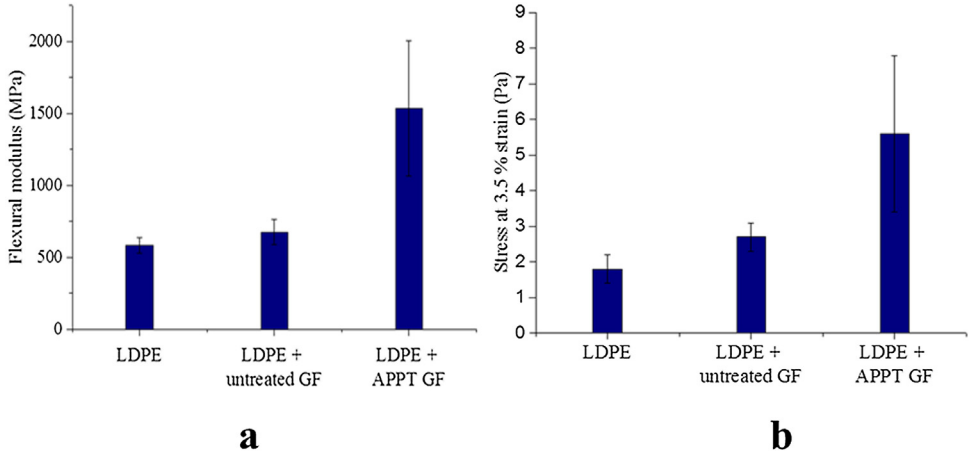

Fig. 9 – Flexural modulus (a) and stress at 3.5% strain (b).

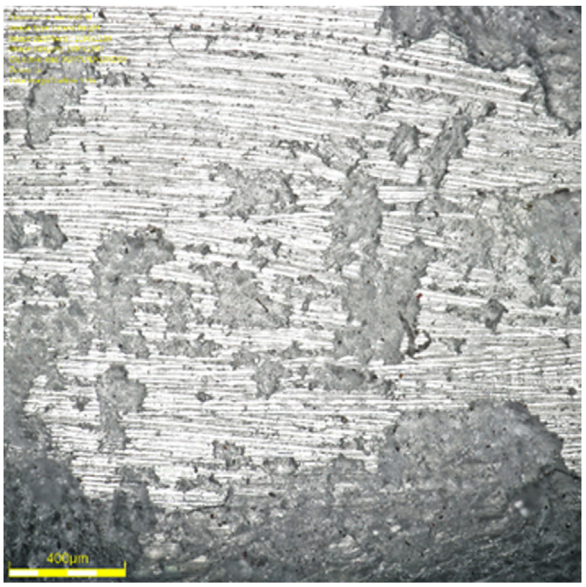

Fig. 10 – Mixed failure obtained in adhesion test.

Table 8 – Absorbed energy and fall speed in drop tower tests.

	Non-reinforced marble	Reinforced marble
Energy (J)	0.59	2.45
Fall speed (m/s)	1.08	2.21

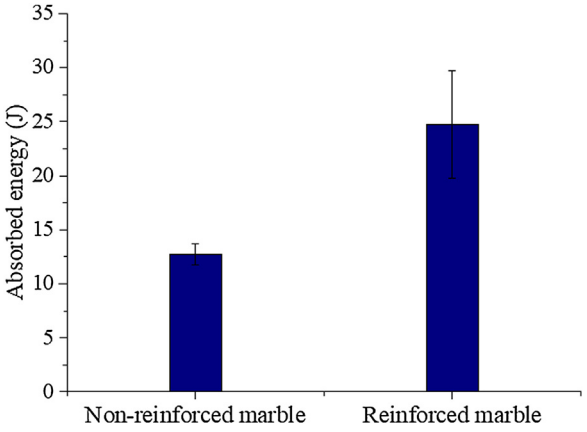

Fig. 11 – Absorbed energy in Charpy test.

fibers, the resistance of the joint is 0.64 ± 0.11 N/mm, and the failure can be seen in Fig. 10.

The joint between marble and composite with treated fibers shows a mixed failure. It can be observed how a part of polyethylene is on the marble surface after the peel test. Adhesion is therefore adequate for the final purpose.

3.2.2. *Impact tests*

From the maximum height in drop tower test, absorbed energy and fall speed are calculated, resulting in the values shown in Table 8. When the reinforcement is adhered to marble, absorbed energy increases by a factor of five, and fall speed doubles. This is due to the good interface between them, and the ability to absorb energy without the breakage of the flexible composite material.

Absorbed energy when the sample breaks can be measured by Charpy test. Energy values with and without reinforcement are shown in Fig. 11. As in drop tower tests, the reinforcement of marble increases drastically the absorbed energy. Furthermore, in Charpy test, the breakage of the sample also changes when marble is reinforced, as can be seen in Fig. 12. The

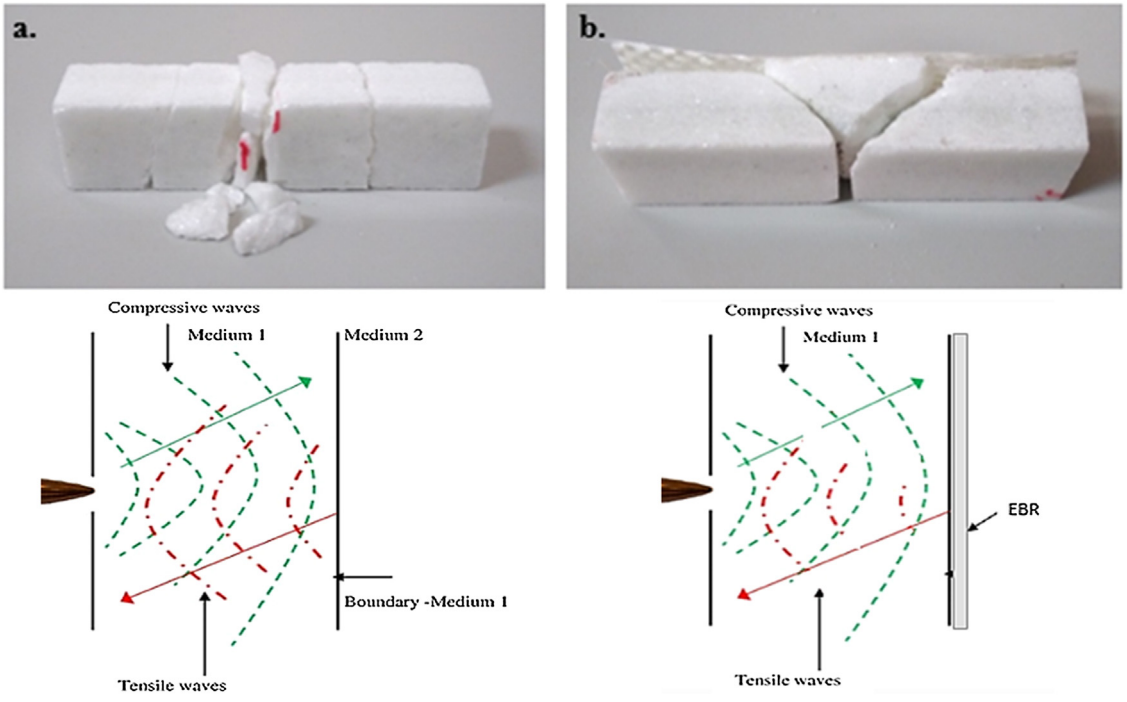

Fig. 12 – Breakage of marble without (a) and with reinforcement (b).

scheme, shown below, presents the efforts generated during the impact in both cases [40]. Marble, like every ceramics, has high compressive strength, but it presents low tensile strength. When the compressive waves travel across, they are reflected like tensile waves, which produces breakage by tensile strength when marble is not reinforced (Fig. 12 down). When the marble is reinforced, the intensity of the tensile waves is lower thanks to the good adhesion between the components of the composite, as well as with the marble piece.

4. Conclusions

- APPT effect on glass fiber surface:
  - Cleaning and etching: these effects are observed by SEM and AFM, where a smoother and more homogeneous surface is found with APPT. Furthermore, by FTIR, a reduction in the amount of wax on the surface is found.
  - Activation: this effect is observed by surface energy measurements, DSC and FTIR. Polar and electron donor groups are introduced in the surface, which act as nucleation points resulting on transcrystallization process.
- GF-LDPE adhesion: by peel, pull-out and pull-off tests an important improvement of the adhesion is observed with plasma treatment.
- Composite flexural properties: the quality of the interface affects the flexural modulus and the strength of composites: the better the interface, the higher these parameters.
- Reinforcement of marble: when marble is reinforced with the composite both, drop tower and Charpy tests, show an important increase in absorbed energy when the material is subjected to an impact. It means that the toughness of the marble increase drastically. It is important to highlight that this increase is achieved thanks to the good adhesion of every interface (matrix-fiber and composite -marble).

Conflicts of interest

The authors declare no conflicts of interest.

Funding

This work was supported by Interreg SUDOE project SOE1/P1/E0307.

REFERENCES

[1] Stewart R. Thermoplastic composites – recyclable and fast to process. Reinf Plast 2011;55:22–8.
[2] Kumar R, Singh R, Ahuja IPS, Penna R, Feo L. Weldability of thermoplastic materials for friction stir welding—a state of art review and future applications. Compos B: Eng 2018;137:1–15.
[3] Yao SS, Jin FL, Rhee KY, Hui D, Park SJ. Recent advances in carbon-fiber-reinforced thermoplastic composites: a review. Compos B: Eng 2018;142:241–50.
[4] Sepe R, Bollino F, Boccarusso, Caputo F. Influence of chemical treatments on mechanical properties of hemp fiber reinforced composites. Compos B: Eng 2018;133:210–7.
[5] Enciso B, Abenojar J, Martinez MA. Influence of plasma treatment on the adhesion between a polymeric matrix and natural fibres. Cellulose 2017;24(4):1791–801.
[6] Iorio M, Santarelli ML, González-Gaitano G, González-Benito J. Surface modification and characterization of basalt fibers as potential reinforcement of concretes. Appl Surf Sci 2018;427:1248–56.
[7] Jing M, Che J, Xu S, Liu X, Fu Q. The effect of surface modification of glass fiber on the performance of poly(lactic acid) composites: graphene oxide vs. silane coupling agents. Appl Surf Sci 2018;435:1046–56.
[8] Savas LA, Tayfun U, Dogan M. The use of polyethylene copolymers as compatibilizers in carbon fiber reinforced high density polyethylene composites. Compos B: Eng 2016;99:188–95.
[9] Liu X, Yang C, Lu Y. Contrastive study of anodic oxidation on carbon fibers and graphite fibers. Appl Surf Sci 2012;258:4268–75.
[10] Zhao X, Xiong D, Wu X. Effects of surface oxidation treatment of carbon fibers on biotribological properties of CF/PEEK materials. J Bionic Eng 2017;14:640–7.
[11] Li VC, Chan YW, Wu HC. In: Interface strengthening mechanisms in polymeric fiber reinforced cementitious composites. Special session honoring Prof. H. Krenchel. BMC4 Proceedings; 1994. p. 7–16.
[12] Grujicic M, Sellappan V, Omar MA, Seyr N, Obieglo A, Erdmann M, et al. An overview of the polymer-to-metal direct-adhesion hybrid technologies for load-bearing automotive components. J Mater Process Technol 2008;197:363–73.
[13] Long D, Guo H, Cui J, Chen X, Lu M. Rapid etching of carbon fiber induced by noble metal nanoparticles. Mater Lett 2017;197:45–7.
[14] Liu Z, Chen P, Han D, Lu F, Yu Q, Ding Z. Atmospheric air plasma treated PBO fibers: wettability, adhesion and aging behaviors. Vacuum 2013;92:13–9.
[15] Schulze K, Hausmann J, Wielage B. The stability of different titanium-PEEK interfaces against water. Procedia Mater Sci 2013;2:92–102.
[16] Martinez MA, Abenojar J, Lopez de Armentia S. Environmentally friendly plasma activation of acrylonitrile–butadiene–styrene and polydimethylsiloxane surfaces to improve paint adhesion. Coatings 2018;8:428, 2018.
[17] Scalici T, Fiore V, Valenza A. Effect of plasma treatment on the properties of Arundo Donax L. Leaf fibres and its bio-based epoxy composites: a preliminary study. Compos B: Eng 2016;94:167–75.
[18] Abenojar J, Martínez MA, Encinas N, Velasco F. Modification of glass surfaces adhesion properties by atmospheric pressure plasma torch. Int J Adhes Adhes 2013;44:1–8.
[19] Sassoni E, Graziani G, Ridolfi G, Bignozzi MC, Franzoni E. Thermal behavior of Carrara marble after consolidation by ammonium phosphate, ammonium oxalate and ethyl silicate. Mater Des 2017;120:345–53.
[20] Tesser E, Lazzarini L, Bracci S. Investigation on the chemical structure and ageing transformations of the cycloapliphatic epoxy resin EP2101 used as stone consolidant. J Cult Herit 2018;31:72–82.
[21] Processing of Marble Slabs and Equipment Requirements, Al Qamer Company for Energy and Infrastructure. [cited 2019 May 20]. Available from: http://www.alqamer.com/index.php/2016-02-01-19-25-41/processing-of-marble.

[22] Bellini C, Polini W, Sorrentino L, Turchetta S. Mechanical performances increasing of natural stone by GFRP sandwich structures. Procedia Struct Integr 2018;9:179–85.
[23] Mofokeng JP, Luyt AS, Tábi T, Kovács J. Comparison of injection moulded, natural fibre-reinforced composites with PP and PLA as matrices. J Thermoplast Compos 2011;25:927–48.
[24] Ludueña L, Vázquez A, Alvarez V. Effect of lignocellulosic filler type and content on the behavior of polycaprolactone based eco-composites for packaging applications. Carbohydr Polym 2012;87:411–21.
[25] Young RJ, Heppenstall-Butler M. Polymer transcrystallinity in composites. Encyclopedia of materials: science and technology. 2nd ed; 2001. p. 7535–40.
[26] Olmos D, Bagdi K, Mózco J, Pukánszky B, González-Benito J. Morphology and interphase formation in epoxy/PMMA/glass fiber composites: effect of molecular weight of the PMMA. J Colloid Interface Sci 2011;360:289–99.
[27] Encinas N, Pantoja M, Abenojar J, Martínez MA. Control of wettability of polymers by surface roughness modification. J Adhes Sci Technol 2010;24:1869–83.
[28] Van Oss CJ, Good RJ, Chaudhury MK. Additive and nonadditive surface tension components and the interpretation of contact angles. Langmuir 1988;4:884–91.
[29] Godara A, Gorbatikh L, Kalinka G, Warrier A, Rochez O, Mezzo L, et al. Interfacial shear strength of a glass fiber/epoxy bonding in composites modified with carbon nanotubes. Compos Sci Technol 2010;70(9):1346–52.
[30] Batista NL, Rezende MC, Botelho EC. Effect of crystallinity on CF/PPS performance under weather exposure: moisture, salt fog and UV radiation. Polym Degrad Stab 2018;153:255–61.
[31] Encinas N, Lavat-Gil M, Dillingham RG, Abenojar J, Martínez MA. Cold plasma effect on short glass fiber reinforced composites adhesion properties. Int J Adhes Adhes 2014;48:85–91.
[32] Encinas N, Abenojar J, Martínez MA. Development of improved polypropylene adhesive bonding by abrasion and atmospheric plasma surface modifications. Int J Adhes Adhes 2012;33:1–6.
[33] Pantoja M, Abenojar J, Martínez MA. Influence of the type of solvent on the development of superhydrophobicity from silane-based solution containing nanoparticles. Appl Surf Sci 2017;397:87–94.
[34] Pantoja M, Abenojar J, Martínez MA, Velasco F. Silane pretreatment of electrogalvanized steels: effect on adhesive properties. Int J Adhes Adhes 2016;65:54–62.
[35] Groβ T, Hermann T, Shi B, Jäger A, Chiu P, Metz P. Further studies on sultones derived from carbine cyclization cycloaddition cascades. Tetrahedron 2015;71(25):5925–31.
[36] Muscat D, Tobin MJ, Guo Q, Adhikari B. Understanding the distribution of natural wax in starch–wax films using synchrotron-based FTIR (S-FTIR). Carbohydr Polym 2014;102:125–35.
[37] Abenojar J, Martínez MA, Velasco F, Rodríguez-Pérez MA. Atmospheric plasma torch treatment of polyethylene/boron composites: effect on thermal stability. Surf Coat Technol 2014;239:70–7.
[38] Seymour RB, Carraher CE Jr. Introducción a la química de los polímeros, 3rd. ed. Reverté; 2002. ISBN: 978-84-291-7926-2.
[39] Arslan C, Dogan M. The effect of silane coupling agents on the mechanical properties of basalt fiber reinforced poly(butylene terephtalate) composites. Compos B: Eng 2018;146:145–54.
[40] Mohotti D, Ngo T, Mendis P, Raman SN. Polyurea coated composite aluminum plates subjected to high velocity projectile impact. Mater Des 2013;52:1–16.